Prepared for submission to JHEP

Impact of Rare Decays $t \to \ell'\nu b\ell\ell$ and $t \to qq'b\ell\ell$ on Searches for Top-Associated Physics

P. Onyisi, A. Webb

Department of Physics, University of Texas at Austin
Austin, TX 78712, United States

E-mail: ponyisi@utexas.edu, awebb@cern.ch

Abstract: Searches for top quark-associated physics such as $t\bar{t}W$ or $t\bar{t}H$ in final states with multiple leptons require a careful accounting of expected backgrounds due to the lack of reconstructible resonances. We demonstrate that the rare top quark decays $t \to \ell'\nu b\ell\ell$ and $t \to qq'b\ell\ell$, when a soft lepton is not detected, can contribute a non-negligible background to such searches. Simulations in the LHC experiments typically do not account for such decays and as such backgrounds to such searches may be underestimated.

arXiv:1704.07343v1 [hep-ph] 24 Apr 2017

Contents

1 Introduction 1

2 Asymmetric Internal Conversion Kinematics 2

3 The Rare Decays $t \to \ell' \nu b \ell \ell$ and $t \to q q' b \ell \ell$ 3

4 Simulation of Rare Top Decay Impact on $3\ell + b$ Searches 5

5 Conclusion 11

1 Introduction

The achievement of 13 TeV center of mass energy and design collision luminosity at the Large Hadron Collider (LHC) will enable a rich program of studies of the production of electroweakly-interacting particles produced in association with the top quark. The processes $pp \to t\bar{t}Z$ and $t\bar{t}W$ are established [1–3], while the production of $t\bar{t}H$ remains to be clearly demonstrated [4–7]. These processes will provide critical information on the coupling of the top quark to electroweak gauge bosons and the mechanism of top quark mass generation.

One of the most powerful ways of accessing $t\bar{t}W$ and $t\bar{t}H$ production is through final states with multiple leptons, especially three leptons or two leptons of the same sign. These lepton requirements are sufficient to suppress contamination from top pair production, where at most two same-sign leptons are expected; $t\bar{t}$ will typically contribute a background only through lepton charge misreconstruction, additional leptons from heavy hadron decay, or $t\bar{t}\gamma$ production with subsequent $\gamma \to e^+e^-$ conversion in detector material. However, since these final states have multiple neutrinos, separation of different processes is complex and simulation of rare processes that mimic the signature can become very important.

The potential relevance of backgrounds with "lost" leptons to multilepton searches was pointed out in the context of the search for $H \to WW^* \to \ell\nu\ell'\nu$ produced in gluon-gluon fusion [8]. The production of $W\gamma^* \to \ell\nu\ell'(\ell')$, where one of the daughters of the virtual photon fails to be reconstructed, can mimic the dilepton signature of Higgs boson production. Such a situation is especially common when $m(\gamma^*)$ is low and the flight directions of the daughter leptons are aligned with the momentum of the virtual photon in the lab frame: one lepton is then often red-shifted to very low momentum in the lab frame and may not pass analysis momentum cuts and not contribute enough isolation energy to cause its pair partner lepton to appear non-isolated. This phenomenon of "asymmetric internal conversion" was found to contribute a non-trivial background to the $H \to WW^*$ search.

In this paper, we demonstrate that a generally-neglected process, $pp \to t\bar{t}$, where one top quark undergoes the rare decay $t \to \ell' \nu b \gamma^*$ or $t \to q q' b \gamma^*$ with subsequent decay $\gamma^* \to \ell\ell$,

can induce a significant background to multilepton searches for top quark-associated phenomena via asymmetric internal conversions. In light of persistent excesses over the Standard Model prediction in $t\bar{t}W$ and $t\bar{t}H$ multilepton searches, potential additional backgrounds are important to identify. Since generally-used QED showering algorithms do not include virtual photon splitting to leptons, this contribution needs to be explicitly included in event generators as a matrix element calculation.

The paper is organized as follows. In Section 2 the generic behavior expected of AIC as a function of the momentum and mass of the virtual photon is discussed. In Section 3 the decay width for the internal conversion decay of a top quark is determined and compared with previous predictions. In Section 4 a realistic detector parametrization is used to study how AIC events will be reconstructed and the resulting yields in a trilepton analysis are compared to those of the $t\bar{t}W$ and $t\bar{t}H$ production processes.

2 Asymmetric Internal Conversion Kinematics

Asymmetric internal conversion (AIC) events $\gamma^* \to \ell\ell$ will leave different observable signatures depending on on $m(\gamma^*)$, $p_T(\gamma^*)$, and the angle θ between the ℓ^- flight direction and the γ^* flight direction as measured in the virtual photon rest frame.

To gain some insight into the kinematics of asymmetric internal conversion events, we run toy Monte Carlo of $\gamma^* \to \mu^+\mu^-$ decays for various values of $m(\gamma^*)$ and $p(\gamma^*)$, mapping the fraction of events that pass two types of selections:

1. A two-lepton selection, where both leptons are required to have momentum above 10 GeV, and to be separated by more than 0.3 radians (isolation);

2. A one-lepton selection, where exactly one lepton must have momentum above 10 GeV, and where, if the two leptons lie within 0.3 radians, the second is required to satisfy $p(\text{sublead})/p(\text{lead}) < 0.1$ (isolation).

In the toy MC, total momentum is used instead of transverse momentum p_T to simplify the problem; they are equivalent for $\eta \approx 0$. For each value of $m(\gamma^*)$ and $p(\gamma^*)$ tested, many potential decay angles $\cos\theta$ are chosen in the rest frame of the virtual photon, and then the system is boosted into the lab frame. The virtual photons are assumed to be completely transversely polarized and therefore are generated according to the probability density

$$P(\cos\theta) = \frac{3}{8}\frac{2 - \beta^2 + \beta^2\cos^2\theta}{1 + \frac{1}{2}(1-\beta^2)}$$

where β is the lepton velocity in the virtual photon rest frame; in the limit of ultrarelativistic lepton daughters this recovers the familiar form $P \propto 1 + \cos^2\theta$. These results only depend on the parameters of the virtual photon system and so are universal for AIC events with transversely polarized photons.

The probability for an event to be chosen under the two selections, as a function of virtual photon mass and momentum, is shown in Figure 1 for the dimuon case. Several features are evident. At high $m(\gamma^*)$ and $p(\gamma^*)$, the two plots are complementary, as at

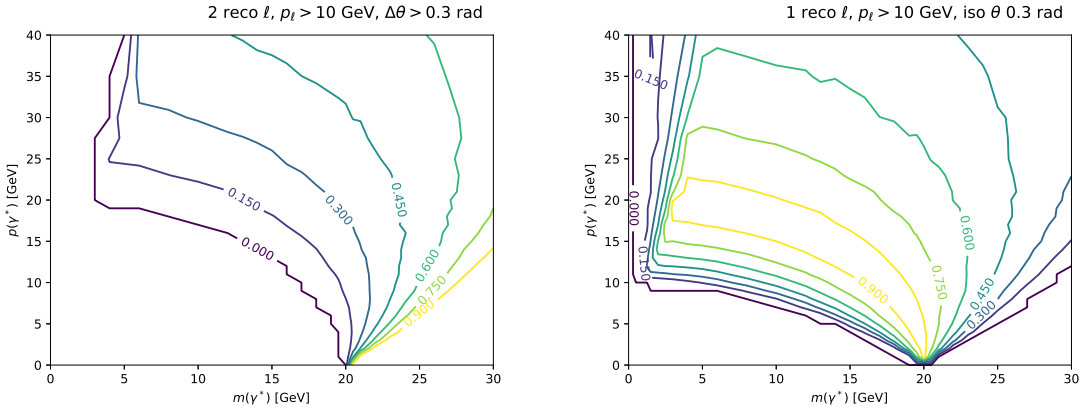

(a) Two lepton selection

(b) One lepton selection

Figure 1: Acceptance for two- and one-lepton selections in asymmetric internal conversion $\gamma^* \to \mu\mu$ events.

least one lepton will have $p > 10$ GeV, and the two selections are disjoint. At low mass and momentum, no leptons are found at all; they are both too soft. At low mass and high momentum, the lepton separation/isolation requirements suppress the acceptance. There is a crescent-shaped region of near-zero dilepton acceptance with over 90% acceptance for the single lepton selection, extending to $m(\gamma^*) \sim 2.5$ GeV; the acceptance is still significant until it is truncated by the isolation cut. We conclude that an analysis that requires one lepton and vetoes a second will have high sensitivity to these "lost" leptons.

We can try to see if there are ways to mitigate this background or to constrain it from data. From Figure 1 it is clear that the acceptance for finding two leptons with $p > 10$ GeV in the region of interest is essentially zero, so we must try other means. First, we ask whether the subthreshold lepton can still be seen, with the leading lepton threshold still at 10 GeV. Figure 2a shows the median momentum of the subleading lepton when exactly one lepton is found with $p > 10$ GeV; if a subleading lepton can be reconstructed down to 4 GeV momentum, then events down to $m(\gamma^*) = 5$ GeV can be reconstructed in most of the dangerous cresecent region, although the very lowest masses cannot be reached.

We also consider the possibility of lowering the leading lepton threshold to 5 GeV and eliminating the separation cut between two reconstructed leptons in order to improve acceptance at low $m(\gamma^*)$. The results are shown in Figure 2b. With this selection, an acceptance of $\gtrsim 30\%$ can be achieved down to dilepton threshold in the dangerous crescent region. The better matching of the shape of the acceptance curve to the crescent in the latter case, and the ability to reach lower $m(\gamma^*)$, suggest it as a preferred solution to map out the cross section for AIC processes in data.

3 The Rare Decays $t \to \ell'\nu b\ell\ell$ and $t \to qq'b\ell\ell$

At 13 TeV, a $\sigma(pp \to t\bar{t})$ of 832 pb has been calculated at NNLO+NNLL using the Top++ v2.0 program [9] by the LHC Top Working Group [10]. By comparison, the $pp \to t\bar{t}W \to$

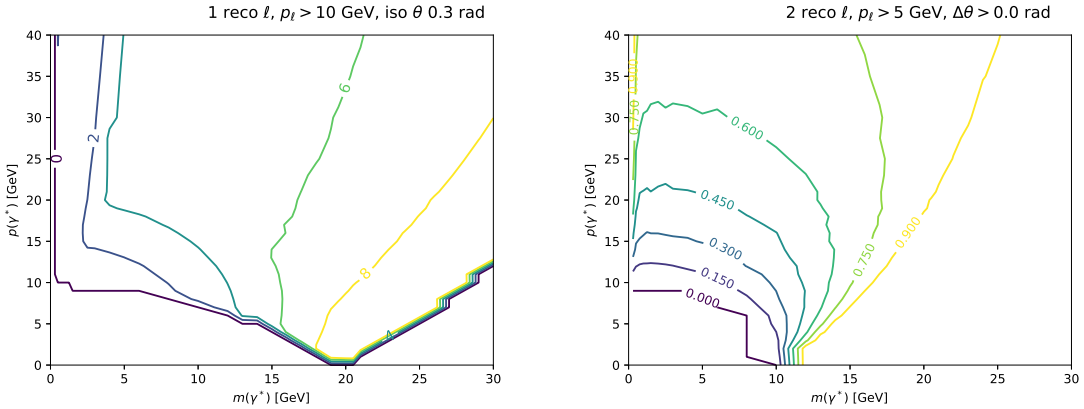

(a) Median subleading lepton momentum in GeV (b) Two lepton acceptance for $p > 5$ GeV selection

Figure 2: (Left) median subleading lepton momentum when only one lepton is found with $p > 10$ GeV; (right) acceptance for two-lepton selection when lepton momentum threshold is lowered to 5 GeV and lepton angular separation requirements are removed.

$3\ell 3\nu bb$ ($\ell = e,\ \mu$) cross section at NLO is 6.2 fb [11, 12], so a 10^{-5} top quark branching fraction to a similar final state could produce comparable yields.

Top quark decays are dominated by the CKM-favored two-body decay $t \to Wb$. Other potential two-body decays are either suppressed by small CKM elements (for Wq) or GIM-suppressed loops (Zq or Hq). The CKM-allowed decay $t \to WZb$ is very near threshold and the decay width is dominated by finite-width effects. Ref. [13] derives a branching fraction $\mathcal{B}(t \to WZb) \sim 2 \times 10^{-6}$ which means this will not compete with $pp \to t\bar{t}Z$ or tZ production. The decays $t \to Wbg$ and $t \to Wb\gamma$ are significant but generally treated as FSR corrections to $t \to Wb$ using QCD and QED Monte Carlo showering algorithms.

The four-body decay $t \to Wb\ell^+\ell^-$ was considered in Ref. [14] and found to give a branching ratio $R = \Gamma(t \to Wbe^+e^-)/\Gamma(t \to Wb) = 6.3 \times 10^{-6}$ for $m(\gamma^*)^2 > 20$ GeV^2, and the same for the dimuon decay (all at leading order). This is clearly in the regime discussed above where this decay might compete with processes such as $t\bar{t}W$, considering in particular that one expects significant cross section below this $m(\gamma^*)$ cutoff of ≈ 4.5 GeV. A leading order calculation suffers from the pole of the photon propagator, especially for the dielectron mode where the branching ratio to the $t \to Wb$ mode exceeds unity with an $m(\gamma^*)^2$ cut less than 10^{-3} GeV^2, which is still above dielectron threshold. One expects these to be compensated by virtual corrections in a higher order calculation and, indeed, the best strategy for for dealing with these decays is most likely a resummed calculation or parton shower. Nevertheless, it is instructive to study the fixed leading order calculation.

We use MadGraph5_aMC@NLO [12] (hereafter MG5_aMC) version 2.5.4, running in leading order mode, to study the inclusive processes $t \to \ell'\nu b\ell\ell$ and $t \to qq'b\ell\ell$. We use $m_t = 173$ GeV and use non-zero lepton masses in the calculation. First, we compute the ratio $R = \Gamma(t \to Wbe^+e^-)/\Gamma(t \to Wb)$ for $m(\gamma^*)^2 > 20$ GeV^2, to compare with Ref. [14]. Our result is 5.8×10^{-6}, in reasonable agreement with the earlier calculation. We find

that increasing the top mass by 0.5 GeV results in an increase in the ratio of 0.08×10^{-6}, indicating good stability with the top quark mass choice.

In the calculation of Ref. [14] the possibility of the virtual photon being radiated from the daughters of the W boson is not considered. Considering the full set of possible diagrams for $t \to (\ell'\nu, qq')be^+e^-$, we compute a somewhat larger R of 1.1×10^{-5} for the same cutoff $m(\ell^+\ell^-)^2 > 20$ GeV^2. (In the case of the three leptons having the same flavor, the $m(\ell\ell)$ threshold is applied on both opposite sign pairs.) We find that $\Gamma(qq'be^+e^-)/\Gamma(\ell'\nu e^+e^-) = 1.2$ summing over all lepton flavors ℓ', which is much smaller than the equivalent ratio $\Gamma(qq'b)/\Gamma(\ell'\nu b) \approx 2$. This feature seems to be robust to various generation options and may arise from a) the smaller charges of the quarks compared to the charged leptons and b) interference between diagrams involving W-daughter radiation and other diagrams. In Section 4 we focus on the $\ell'\nu b\ell^+\ell^-$ case and so are not sensitive to potential complications in W hadronic decays.

For the simulations of Section 4 we choose a lower $m(\ell^+\ell^-)$ threshold, 1 GeV. This allows us to fully populate the high-acceptance region for AIC events. The corresponding R is 4.9×10^{-5}. The simulation of $t\bar{t}$ events with a rare decay is performed completely at LO in MG5_aMC, with the rare decays simulated as a 5-body decay. Although this simulation will miss features such as recoil of the $t\bar{t}$ system against hard additional jets, it will illustrate the core physics. We strongly emphasize that higher-order corrections are expected to induce large corrections and that in the leading order calculation there is a large additional cross section at $m(\gamma^*) < 1$ GeV. This R value should therefore be treated as purely indicative.

4 Simulation of Rare Top Decay Impact on $3\ell + b$ Searches

To give a practical picture of the potential impact of these rare top decays on an actual search, we consider a simplified $3\ell + b$ search with a Z-veto. This final state is sensitive to $t\bar{t}W$ and $t\bar{t}H$.

The sensitivity of such an analysis to asymmetric conversions depends strongly on detector response and analysis choices. We pass events generated in MG5_aMC at 13 TeV and showered by Pythia 8 [15, 16] to the generic detector fast simulation program Delphes [17], which was configured to approximate the characteristics of the CMS detector. We generate three different processes. The $t\bar{t}$ rare decays produce the final state $\ell_1^+\nu_1 b\ell_2^-\bar{\nu}_2\bar{b}\ell_3^+\ell_3^-$, where all leptons are either e or μ and the $\ell_3^+\ell_3^-$ pair can come from the decay of either t or $\bar{t}$. The $pp \to t\bar{t}W$ process is generated with subsequent decay of all W bosons to a lepton and a neutrino, where here leptons include e, μ, and τ. The $pp \to t\bar{t}H$ process is generated with subsequent $H \to WW^*$ decay; three of four W bosons are required to decay to a lepton and neutrino (including e, μ, and τ) and the fourth is required to decay to qq'. For $t\bar{t}$ we assign a cross section of 10.9 fb using a branching fraction $\mathcal{B}(t \to \ell'\nu b\ell\ell)$ computed using MG5_aMC and a total inclusive $t\bar{t}$ cross section of 832 fb. For $t\bar{t}W$ and $t\bar{t}H$ we assign cross sections of 20.8 and 10.3 fb, respectively, derived from production cross sections and decay branching fractions in the LHC Higgs Cross Section Working Group Yel-

low Report 4 [11] and the Particle Data Group averages [18]. All processes are generated at leading order with no additional partons produced in the matrix element.

The default DELPHES CMS simulation card was altered to use anti-k_T $R = 0.4$ jets with a p_T threshold of 25 GeV, and to require that all reconstructed leptons satisfy $p_T > 10$ GeV. Leptons are required to be isolated; a particle flow algorithm is used to classify additional activity in a cone of $\Delta R \equiv \sqrt{\Delta\eta^2 + \Delta\phi^2} = 0.3$ around the lepton, and the total transverse energy of particles with $p_T > 0.5$ GeV in this cone is required to be less than 10% of the lepton p_T. To remove quarkonia decaying to muon pairs, typical analyses will require that the invariant mass of any opposite sign same flavor lepton pairs to exceed 12 GeV, which will also have the advantage of removing low mass internal conversion events where both leptons are reconstructed.

We consider three possible analysis selection scenarios:

1. exactly three reconstructed leptons with $p_T > 10$ GeV, no further selection on jets;
2. exactly three reconstructed leptons with $p_T > 20$ GeV, no further selection on jets;
3. exactly three reconstructed leptons with $p_T > 20$ GeV, with ≥ 4 jets required.

These are motivated by different potential analysis targets. Scenario 1 illustrates generic features of the different processes and might be used as a preselection for a multivariate discriminant analysis that seeks as much acceptance as possible. Scenario 2 attempts to reduce the impact of the $t\bar{t}$ rare decay background by raising lepton momentum thresholds (this would also be motivated by reducing the contamination from leptons from b- and c-hadron decays), and would be a starting point for a $t\bar{t}W$ selection. Scenario 3 is closest to a selection targeting $t\bar{t}H$, requiring high jet multiplicity to suppress the $t\bar{t}W$ contribution. In all cases triggering should be very efficient and is not considered.

We make no specific selection on the number of b-tagged jets. All three samples ($t\bar{t}$ rare decay, $t\bar{t}W$, $t\bar{t}H$) have virtually identical distributions of the number of reconstructed b-tagged jets, consistent with the tagging efficiency implemented in the DELPHES card. To improve statistical yields for comparisons we do not cut on this variable.

The results for Scenario 1 are shown in Figures 3 and 4. Figure 3a shows the transverse momentum spectrum for the two leptons with the same charge. In the case of the $t\bar{t}$ rare decay with one AIC lepton lost, the AIC lepton that is found will necessarily be one of these same-charge leptons. The large contribution of lower-momentum leptons in the rare decay is clear. Figure 3b shows the same for the one lepton of opposite charge to the other two; this is expected to never come from a conversion, and indeed no low-p_T peak is seen. (In fact the $t\bar{t}H$ process has a larger fractional contribution from the lowest p_T leptons, due to the decay of the low mass offshell W^*.) Figures 3c and 3d show the distributions for the smaller and larger of the two possible invariant masses formed between opposite charge leptons in each event. In both cases the $t\bar{t}$ rare decay distribution looks similar to that of $t\bar{t}H$ and softer than the spectrum for $t\bar{t}W$. The number of jets is shown in Figure 3e; this peaks at 2 for the $t\bar{t}$ rare decays. The spectrum for $t\bar{t}W$ is similar, and $t\bar{t}H$ peaks towards higher multiplicity. Figure 3f shows the ratio of the isolation p_T to the lepton p_T. Although this shows some slope difference between the rare decay and $t\bar{t}W/t\bar{t}H$, this appears to arise

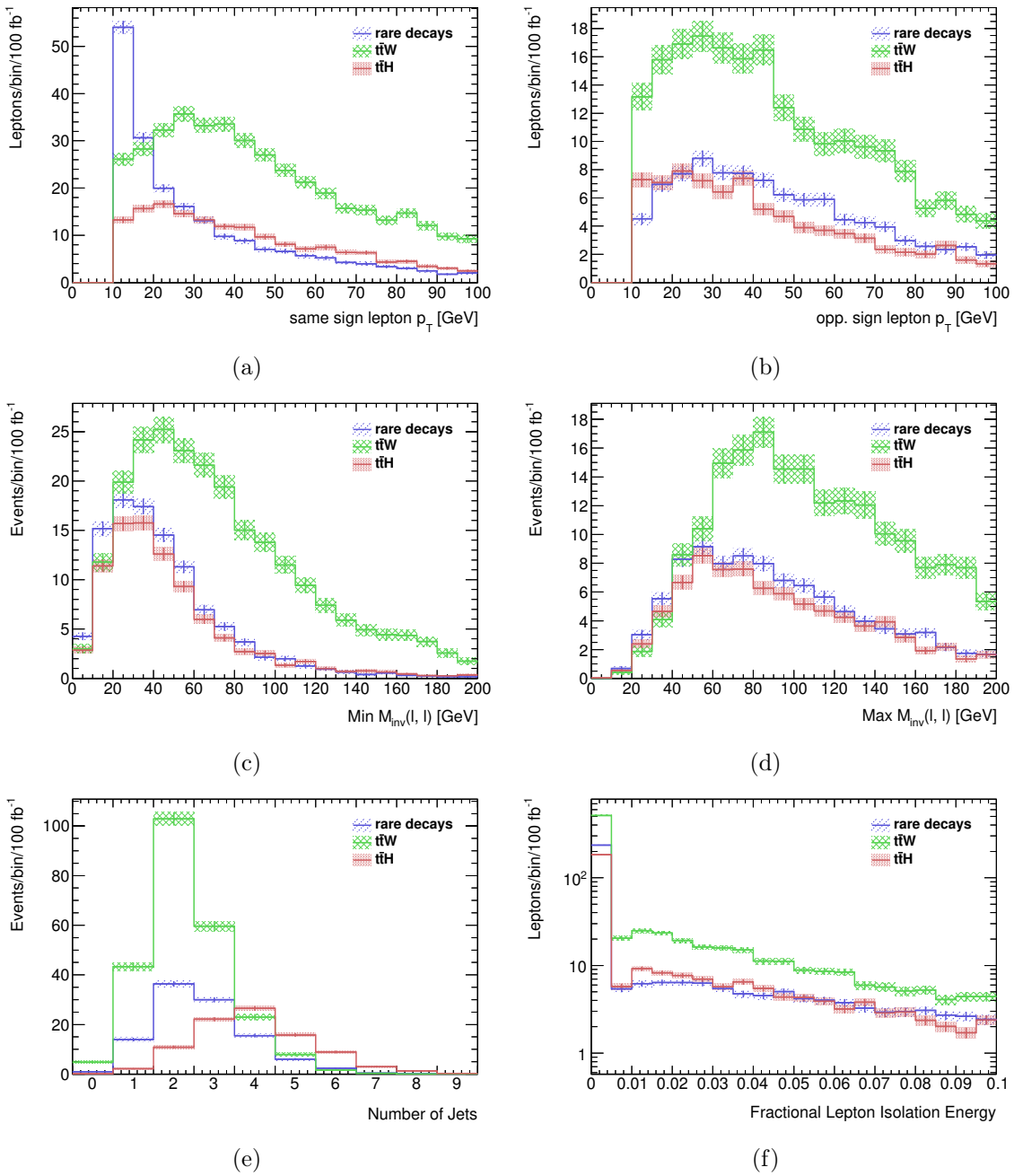

Figure 3: Plots for various variables in the Scenario 1 selection: a) p_T of the two selected leptons of the same charge; b) p_T of the selected lepton of opposite charge to the other two; c) the smaller of the two possible opposite sign dilepton masses $M(\ell^+\ell^-)$; d) the larger of the two possible opposite sign dilepton masses $M(\ell^+\ell^-)$; e) number of reconstructed jets with $p_T > 25$ GeV; f) ratio of isolation p_T in a cone of 0.3 around the lepton to the lepton p_T. Yields are scaled to 100 fb^{-1}. Error bands correspond to statistical uncertainties in the simulated samples.

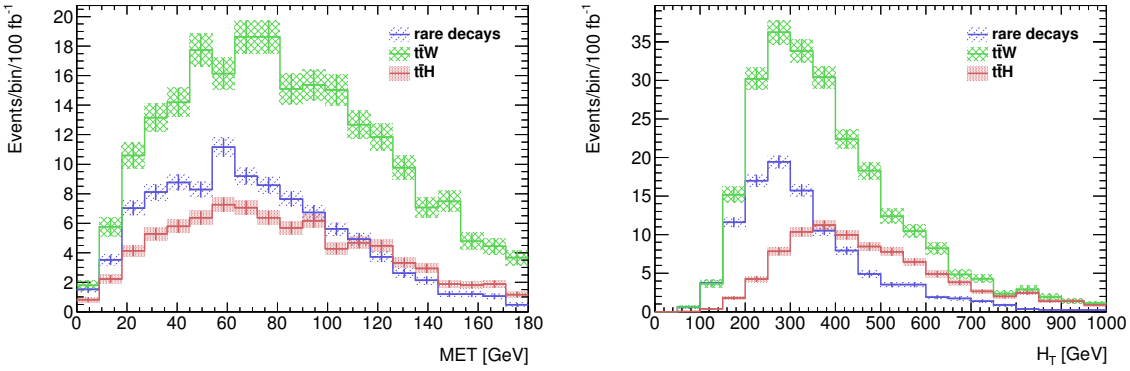

(a) (b)

Figure 4: Additional plots for various variables in the Scenario 1 selection: a) missing transverse energy; b) scalar sum of transverse momenta H_T. Error bands correspond to statistical uncertainties in the simulated samples.

primarily from the different spectrum of the lepton p_T which appears in the denominator, rather than any difference in the isolation energy itself. Finally, Figures 4a and 4b show the missing transverse energy and scalar sum of transverse momenta H_T; the three processes are not dramatically different in these distributions, although $t\bar{t}H$ has a larger H_T consistent with having more jets in the final state.

Typically, to suppress non-prompt lepton contributions, the p_T threshold on the leptons will be higher than 10 GeV. In Scenario 2 we apply a uniform 20 GeV cut on all leptons. (In principle one can do this for the same sign pair only, but the conclusions are the same.) The results are shown in Figure 5 for certain selected variables. The $pp \to t\bar{t}W$ process is now strongly enhanced over both the rare $t\bar{t}$ decay and $t\bar{t}H$ production. Figure 5a shows the p_T of the same-charge leptons. The distribution shows a kink at $\approx$ 40 GeV for the rare decay, above which it has a very similar momentum spectrum to that of $t\bar{t}H$. The invariant mass distributions in Figures 5c and 5d look almost identical between the rare decay process and $t\bar{t}H$; the two processes are distinguished by the number of associated jets and the H_T. Now that the low-p_T spike in the rare decay has been removed, the isolation energy ratio (Figure 5f) looks very similar for all processes.

Finally, we make a requirement on the total number of jets in order to isolate $t\bar{t}H$ and separate it from $t\bar{t}W$. Some variables are shown in Figure 6. Other than in the shape of the same-sign lepton p_T, where the same kink at 40 GeV is seen as in Scenario 2, it is hard to convincingly discriminate the rare decay and $t\bar{t}H$.

The yields of the three considered processes under each scenario are shown in Table 1. In Scenarios 2 and 3 ($t\bar{t}W$- and $t\bar{t}H$-search-like regions) the $t\bar{t}$ AIC background contributes 15–20% of the relevant signal yield, and can have a non-trivial impact on extraction of $t\bar{t}W$ and $t\bar{t}H$ cross sections. Due to the large uncertainty in the branching fraction for the rare decay, this impact may in fact be larger than seen here.

We raise one additional concern. The rare decay process will also appear in same-sign

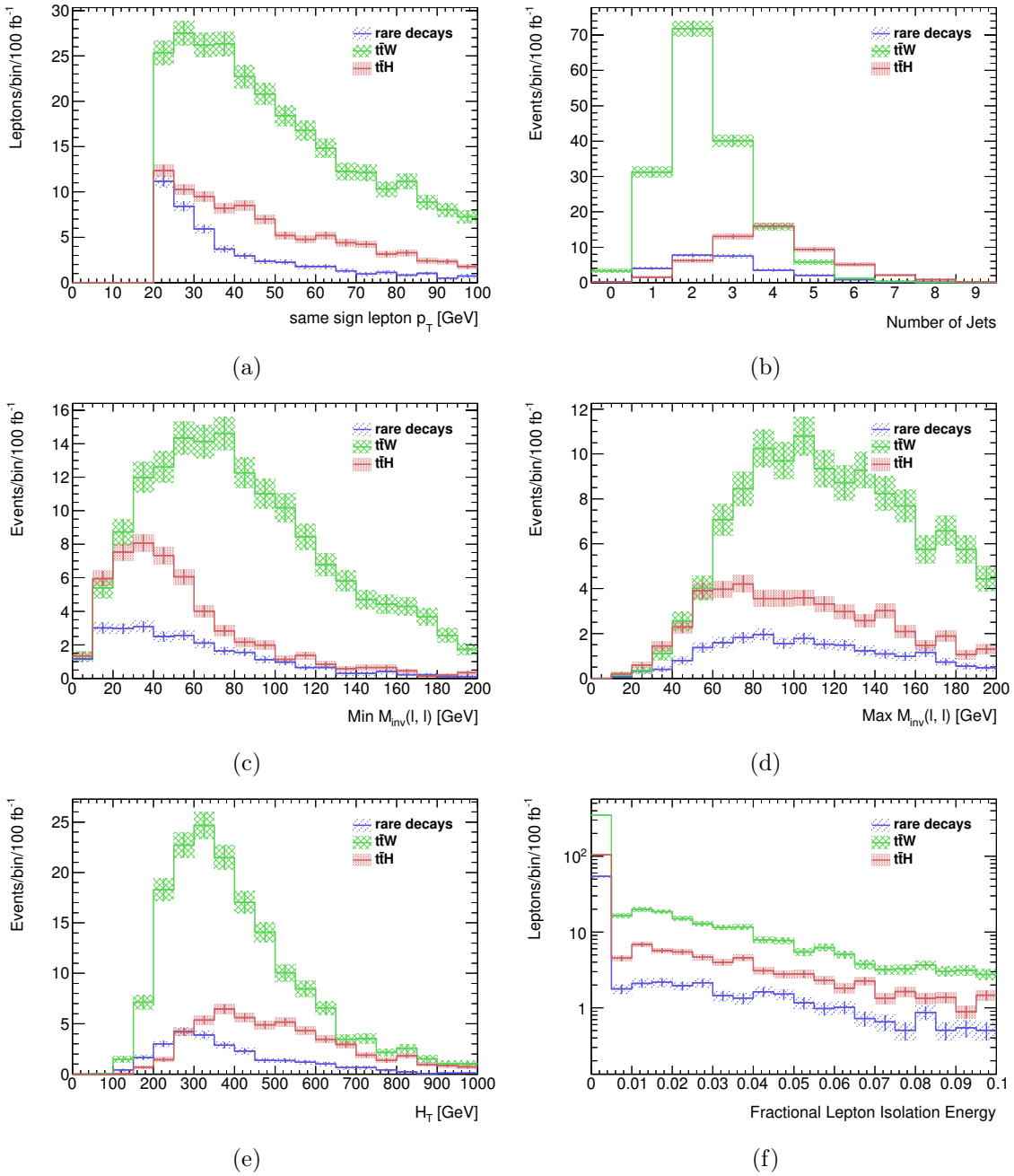

Figure 5: Plots for various variables in the Scenario 2 selection: a) p_T of the two selected leptons of the same charge; b) number of reconstructed jets with $p_T > 25$ GeV; c) the smaller of the two possible opposite sign dilepton masses $M(\ell^+\ell^-)$; d) the larger of the two possible opposite sign dilepton masses $M(\ell^+\ell^-)$; e) scalar sum of transverse momenta H_T; f) ratio of isolation p_T in a cone of 0.3 around the lepton to the lepton p_T. Yields are scaled to 100 fb^{-1}. Error bands correspond to statistical uncertainties in the simulated samples.

dilepton analyses, as the AIC lepton is not charge-correlated with the leptons from W decay

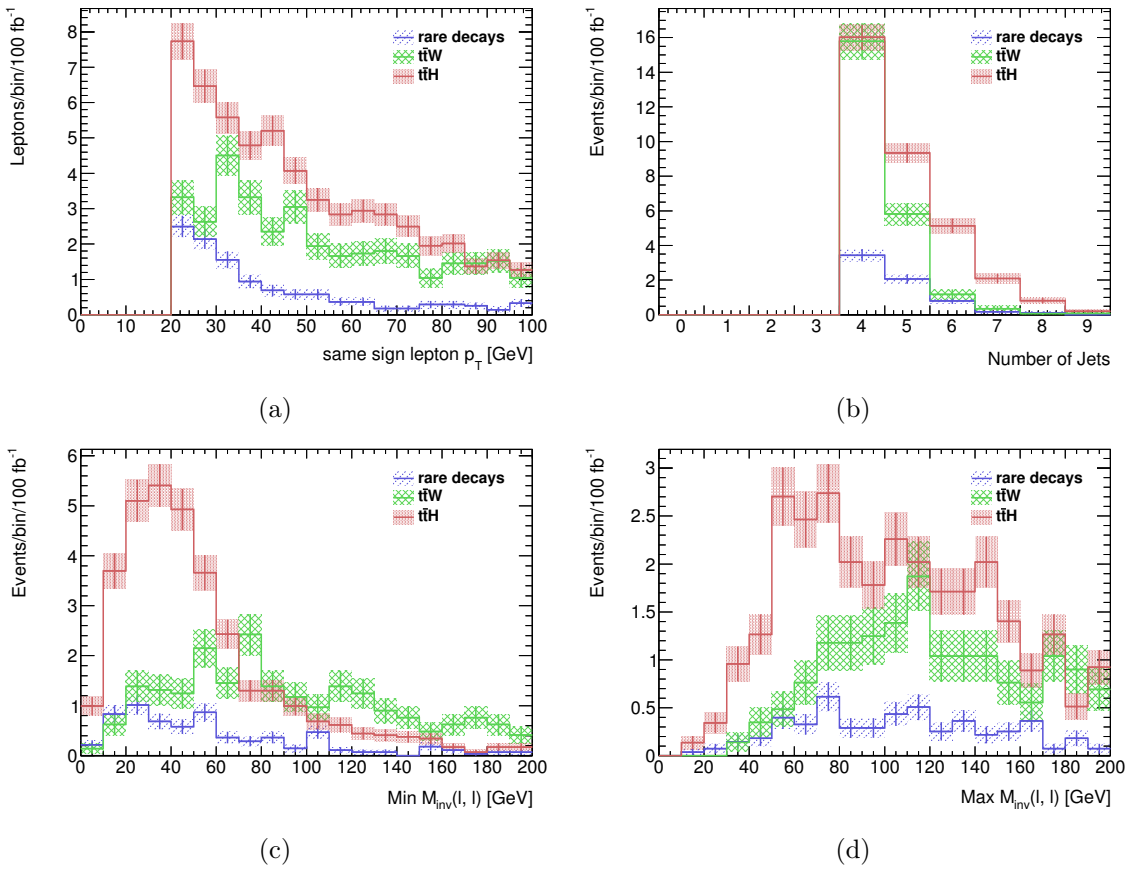

Figure 6: Plots for various variables in the Scenario 3 selection: a) p_T of the two selected leptons of the same charge; b) number of reconstructed jets with $p_T > 25$ GeV; c) the smaller of the two possible opposite sign dilepton masses $M(\ell^+\ell^-)$; d) the larger of the two possible opposite sign dilepton masses $M(\ell^+\ell^-)$. Yields are scaled to 100 fb^{-1}. Error bands correspond to statistical uncertainties in the simulated samples.

Table 1: Expected yields in 100 fb^{-1} of 13 TeV data for rare $t\bar{t}$ decay with asymmetric internal conversion, $t\bar{t}W$, and $t\bar{t}H$ under three different trilepton selections, detailed in the text. The rare decay contribution is normalized to a total production rate of 10.9 fb and has large uncertainties coming from higher-order corrections and the virtual photon invariant mass cutoff.

Selection	$t\bar{t}$ rare decay	$t\bar{t}W$	$t\bar{t}H$
Scenario 1	106	244	91
Scenario 2	26	170	54
Scenario 3	6.6	23	34

in top events. The AIC leptons will appear as a relatively low p_T contribution, and may be hard to distinguish from non-prompt electrons and muons from hadronic decays that happen to be isolated. Extractions of fake factors and validation of data-driven non-prompt

estimates may be affected if this additional prompt lepton contribution is not considered.

5 Conclusion

The rare top decays $t \to (\ell'\nu, qq')b\ell\ell$ have not generally been considered as potential backgrounds for searches. However, at low $\ell\ell$ invariant mass, lepton kinematics and analysis selections can result in a high likelihood of one of the two leptons being reconstructed; the relatively high top decay branching fraction in this region may yield a significant number of events in signal regions for ttW or ttH production. Considering the fact that there are persistent excesses in $t\bar{t}W$ and $t\bar{t}H$ results over the Standard Model expectations in multilepton searches, this background source should be carefully evaluated for its impact in real LHC analyses. A reliable calculation of the decay branching fraction and kinematics, with a proper treatment of the IR divergence as $m(\ell\ell) \to 0$, will be extremely valuable. A degree of data-driven background estimation is possible, requiring the use of soft leptons with momentum down to ≈ 5 GeV to fully reconstruct symmetric internal conversion events.

Acknowledgments

We wish to thank Can Kılıç for invaluable discussion about implementing the rare decays in MG5_aMC. We also thank Tamara Vazquez Schröder and Josh McFayden for input and advice. This work was supported by the US Department of Energy, Office of Science, Office of High Energy Physics, under Award Number DE-SC0007890. This work used the Extreme Science and Engineering Discovery Environment (XSEDE) [19], which is supported by US National Science Foundation grant number ACI-1548562. The authors acknowledge the Texas Advanced Computing Center (TACC) at the University of Texas at Austin for providing HPC resources that contributed to the results in this paper.

References

[1] ATLAS Collaboration, *Measurement of the $t\bar{t}W$ and $t\bar{t}Z$ production cross sections in pp collisions at $\sqrt{s} = 8$ TeV with the ATLAS detector*, *JHEP* **1511** (2015) 172, [1509.05276].

[2] ATLAS Collaboration, *Measurement of the $t\bar{t}Z$ and $t\bar{t}W$ production cross sections in multilepton final states using 3.2 fb^{-1} of pp collisions at $\sqrt{s} = 13$ TeV with the ATLAS detector*, *Eur. Phys. J.* **C77** (2017) 40, [1609.01599].

[3] CMS Collaboration, *Observation of top quark pairs produced in association with a vector boson in pp collisions at $\sqrt{s} = 8$ TeV*, *JHEP* **1601** (2016) 096, [1510.01131].

[4] CMS Collaboration, *Search for the associated production of the Higgs boson with a top-quark pair*, *JHEP* **1409** (2014) 087, [1408.1682].

[5] ATLAS Collaboration, *Search for the Standard Model Higgs boson decaying into $b\bar{b}$ produced in association with top quarks decaying hadronically in pp collisions at $\sqrt{s} = 8$ TeV with the ATLAS detector*, *JHEP* **1605** (2016) 160, [1604.03812].

[6] ATLAS Collaboration, *Search for the associated production of the Higgs boson with a top quark pair in multilepton final states with the ATLAS detector*, *Phys. Lett. B* **749** (2015) 519, [1506.05988].

[7] ATLAS and CMS Collaborations, *Measurements of the Higgs boson production and decay rates and constraints on its couplings from a combined ATLAS and CMS analysis of the LHC pp collision data at $\sqrt{s} = 7$ and 8 TeV*, *JHEP* **1608** (2016) 045, [1606.02266].

[8] R. C. Gray, C. Kılıç, M. Park, S. Somalwar and S. Thomas, *Backgrounds To Higgs Boson Searches from $W\gamma^* \to l\nu l(l)$ Asymmetric Internal Conversion*, 1110.1368.

[9] M. Czakon and A. Mitov, *Top++: A Program for the Calculation of the Top-Pair Cross-Section at Hadron Colliders*, *Comput. Phys. Commun.* **185** (2014) 2930, [1112.5675].

[10] https://twiki.cern.ch/twiki/bin/view/LHCPhysics/TtbarNNLO.

[11] D. de Florian et al., *Handbook of LHC Higgs Cross Sections: 4. Deciphering the Nature of the Higgs Sector*, 1610.07922.

[12] J. Alwall et al., *The automated computation of tree-level and next-to-leading order differential cross sections, and their matching to parton shower simulations*, *JHEP* **1407** (2014) 079, [1405.0301].

[13] G. Altarelli, L. Conti and V. Lubicz, *The $t \to WZb$ decay in the standard model: A Critical reanalysis*, *Phys. Lett.* **B502** (2001) 125, [hep-ph/0010090].

[14] N. Quintero, J. L. Diaz-Cruz and G. Lopez Castro, *Lepton pair emission in the top quark decay $t \to bW^+\ell^-\ell^+$*, *Phys. Rev.* **D89** (2014) 093014, [1403.3044].

[15] T. Sjöstrand, S. Mrenna and P. Skands, *A brief introduction to PYTHIA 8.1*, *Comput. Phys. Commun.* **178** (2008) 852, [0710.3820].

[16] T. Sjostrand, S. Mrenna and P. Skands, *PYTHIA 6.4 Physics and Manual*, *JHEP* **0605** (2006) 026, [hep-ph/0603175].

[17] J. de Favereau, C. Delaere, P. Demin, A. Giammanco, V. Lemaître, A. Mertens et al., *DELPHES 3, A modular framework for fast simulation of a generic collider experiment*, *JHEP* **1402** (2014) 057, [1307.6346].

[18] C. Patrignani et al., *Review of Particle Physics*, *Chin. Phys.* **C40** (2016) 100001.

[19] J. Towns, T. Cockerill, M. Dahan, I. Foster, K. Gaither, A. Grimshaw et al., *XSEDE: Accelerating scientific discovery*, *Computing in Science & Engineering* **16** (2014) 62.